RSC Advances

PAPER

View Article Online
View Journal | View Issue

Cite this: *RSC Adv.*, 2021, **11**, 25951

Large-scale synthesis of a monophosphonated tetrathiatriarylmethyl spin probe for concurrent *in vivo* measurement of pO_2, pH and inorganic phosphate by EPR†

Teresa D. Gluth,‡[ab] Martin Poncelet,‡[ab] Stephen DeVience,[bc] Marieta Gencheva,[bc] Emily. H. Hoblitzell,[bd] Valery V. Khramtsov,[bc] Timothy D. Eubank[bd] and Benoit Driesschaert*[ab]

Received 11th June 2021
Accepted 21st July 2021

DOI: 10.1039/d1ra04551b

rsc.li/rsc-advances

Low-field electron paramagnetic resonance spectroscopy paired with **pTAM**, a mono-phosphonated triarylmethyl radical, is an unmatched technique for concurrent and non-invasive measurement of oxygen concentration, pH, and inorganic phosphate concentration for *in vivo* investigations. However, the prior reported synthesis is limited by its low yield and poor scalability, making wide-spread application of **pTAM** unfeasible. Here, we report a new strategy for the synthesis of **pTAM** with significantly greater yields demonstrated on a large scale. We also present a standalone application with user-friendly interface for automatic spectrum fitting and extraction of pO_2, pH, and $[P_i]$ values. Finally, we confirm that **pTAM** remains in the extracellular space and has low cytotoxicity appropriate for local injection.

Low-field Electron Paramagnetic Resonance (EPR) with the use of a molecular spin probe is a powerful technique to non-invasively measure important physiological parameters in a living animal.[1–4] EPR combines high sensitivity and good penetration depth. Stable tetrathiatriarylmethyl radicals (TAMs or trityls) are ideal spin probes for *in vivo* EPR applications. They exhibit unprecedented stability *in vivo* and ultra-narrow line-widths, which result in a high signal-to-noise ratio.[5] TAM structures with spectral sensitivity to oxygen,[6] pH,[7,8] thiol concentration,[9,10] microviscosity,[11] ROS,[12–14] or redox[15,16] have been developed. We recently reported on a mono-phosphonated tetrathiatriarylmethyl radical **pTAM** (Fig. 1) whose EPR spectrum is sensitive to multiple parameters, namely oxygen concentration, pH, and inorganic phosphate concentration, $[P_i]$.[17–20] This multifunctional probe was utilized to profile the tumor microenvironment (TME) in various mouse models of cancer.[19] The unmatched capability to measure $[P_i]$ has resulted in the identification of this biomarker as a new TME marker for tumor progression.[19] Moreover, the ability to measure pO_2, pH, and $[P_i]$ concurrently using the same probe allows for the direct correlation of these important parameters independent of the probe distribution, providing insight into the biological processes occurring in the TME.

While this spin probe has proven to be of great importance for the study of tissue microenvironment *in vivo*, its current synthesis suffers from a very low yield. Indeed, the published synthesis[17] (Scheme 1) uses a lithiation of tetrathiatriarylmethanol **1** and subsequent reaction with a (2 : 1) mixture of diethyl carbonate and diethyl chlorophosphate. This reaction leads to a statistical mixture of mono-, di- and tri-phosphonated tetrathiatriarylmethanol **2n** that requires tedious purification and drastically decreases the yield of the desired **2b**. After hydrolysis of the ethyl esters using sodium hydroxide and deprotection of the phosphonic acid by TMSBr, the final **pTAM** probe was isolated with a yield of less than 5% from **1**. The published procedure allowed for isolating milligram quantity of the probe for limited *in vivo* studies.[19] However, more extensive utilization of this probe would require a synthetic method that enables gram-scale synthesis of **pTAM**.

Hereby we report an efficient protocol for the large-scale production of the **pTAM** probe as well as a MATLAB application for the automatic fitting of the EPR spectra and determination of the physiological parameters, namely pH, pO_2, and $[P_i]$. Our new strategy takes advantage of a reaction of *ipso* nucleophilic substitution of an aromatic hydrogen or a carboxyl

[a]*Department of Pharmaceutical Sciences, West Virginia University, School of Pharmacy, Morgantown, WV, 26506, USA. E-mail: Benoit.driesschaert@hsc.wvu.edu*
[b]*In Vivo Multifunctional Magnetic Resonance Center, Robert C. Byrd Health Sciences Center, West Virginia University, Morgantown, WV, 26506, USA*
[c]*Department of Biochemistry, West Virginia University, School of Medicine, Morgantown, WV, 26506, USA*
[d]*Department of Microbiology, Immunology, and Cell Biology, West Virginia University, School of Medicine, Morgantown, WV, 26506, USA*

† Electronic supplementary information (ESI) available: Synthetic procedures, analysis, calibration, *in vivo* and cells experiments. See DOI: 10.1039/d1ra04551b

‡ These authors contributed equally.

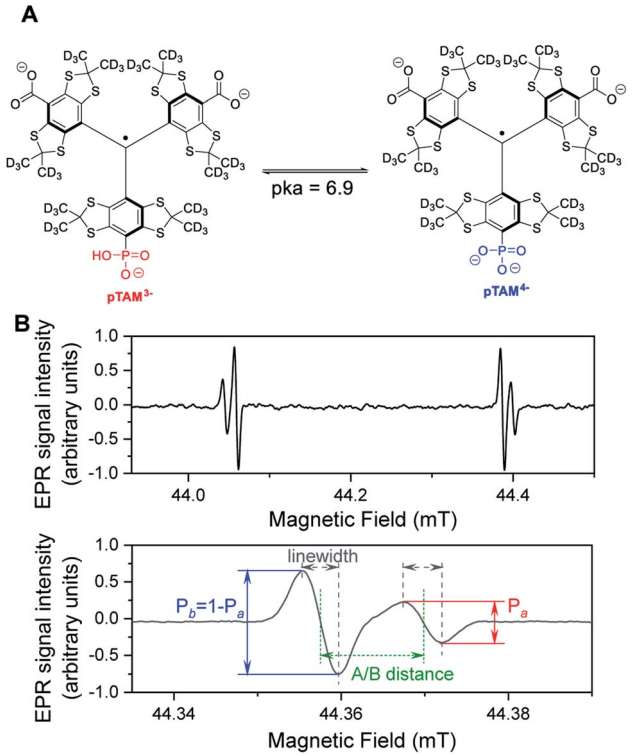

Fig. 1 (A) Structure of **pTAM** spin probe and ionic forms at physiological pH. (B) L-band full spectrum (top) of **pTAM** at pH = 7.13 showing both ionic forms present in the spectrum and zoom on the high field component (bottom). The molar fraction of the acidic form P_a *versus* basic form P_b is a function of the pH of the solution while the linewidths are functions of the oxygen concentration. Inorganic phosphate modulates the exchange rate between the two ionic forms and the *A*/*B* distance. Spectral simulation allows the three parameters to be extracted from the spectrum.

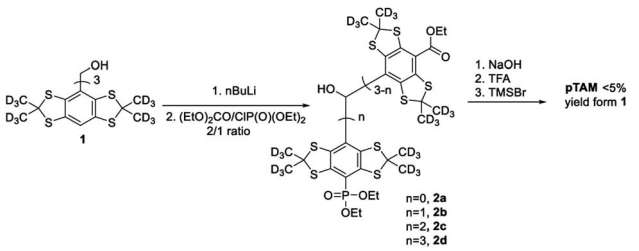

Scheme 1 The first reported synthesis of **pTAM** from **1**.[17]

group on tetrathiatriarylmethyl derivatives reported previously.[21,22] Our synthesis starts with the deuterated Finland trityl (**dFT**) which can be synthesized at large scale without chromatography (Fig. 2A).[23–25] The one-electron oxidation of **dFT** with one equivalent of potassium hexachloroiridate(IV), K_2IrCl_6, in water leads to the trityl carbocation **dFT**$^+$, which is immediately treated with ten equivalents of trimethyl phosphite. The nucleophilic addition of the phosphite in the *para*-position of the aryl ring triggers an oxidative decarboxylation, leading to the mono-phosphonic ester **pTAM-(OMe)$_2$** in 35% conversion, as determined by HPLC/MS (Fig. 2B and S6†). Importantly, the HPLC/MS chromatogram shows that **dFT** radical was also

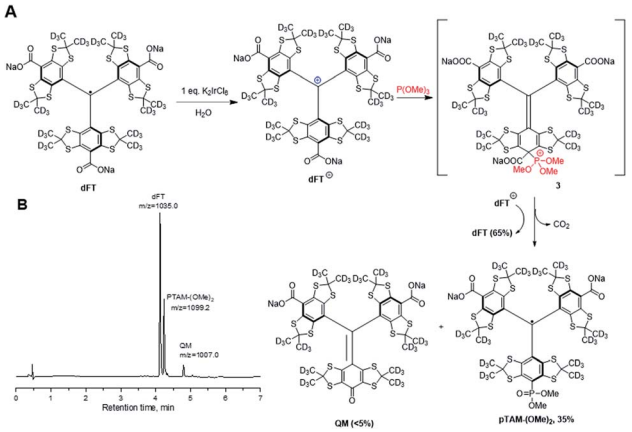

Fig. 2 (A) Synthesis of **pTAM-(OMe)$_2$** from **dFT** and (B) HPLC/MS chromatogram and *m*/*z* ratio of the products after addition of $P(OMe)_3$.

generated back from the trityl carbocation **dFT**$^+$ in 65% yield, consistent with preferential oxidation of intermediate **3** by **dFT**$^+$ in line with previous reports.[21,22] **dFT** can therefore be recycled for future reactions. In addition, <5% of quinone methide (**QM**) was also generated from the nucleophilic addition of water on the trityl cation (see ESI† for mechanism). The use of additional equivalents of K_2IrCl_6 did not increase the yield of **pTAM-(OMe)$_2$** but did lead to higher conversion to the **QM**, TAMs with multiple phosphonates, and unidentified products. The preferential oxidation of **3** by **dFT**$^+$ explains 50% of the back conversion of the trityl radical from the cation. The slightly higher formation of **dFT** observed (65%) could be the result of the direct reduction of the trityl cation by the trimethyl phosphite.

The mono-phosphonated derivatives **pTAM-(OMe)$_2$**, and **dFT** can be separated using a C18 column in 30% and 60% yield, respectively. Finally, the phosphonic acid was deprotected by treatment of **pTAM-(OMe)$_2$** with TMSBr in 95% yield (Scheme 2).

However, for a multigram scale, we found the separation of **dFT** and **pTAM-(OMe)$_2$** to be more challenging. The use of other phosphites with longer alkyl chains (triethyl-, triallyl- or tributyl phosphite), allowed for easier purification but led to smaller conversion (15–25%). On a large scale (tens of grams), the quantitative esterification of the carboxylic acids using methyl iodide and sodium carbonate in DMF directly on the **dFT**/**pTAM-(OMe)$_2$** mixture (Scheme 3) allowed for easy purification by flash chromatography on silica gel. The esterified **pTAM-(OMe)$_4$** was isolated in 35% yield from **dFT** starting material

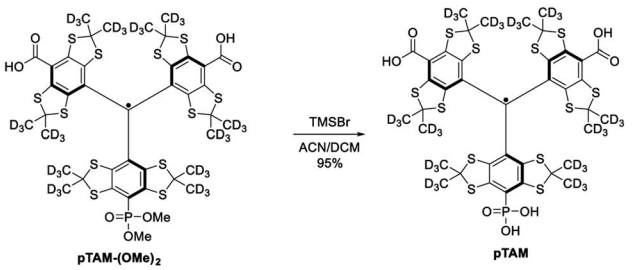

Scheme 2 Deprotection of the phosphonic acid leading to **pTAM**.

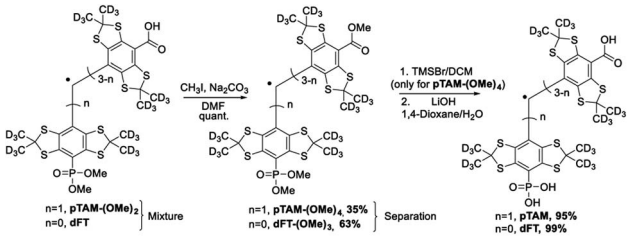

Scheme 3 Esterification of the carboxyl groups to allow for large-scale separation of **pTAM-(OMe)$_4$** and **dFT-(OMe)$_3$**. Then the carboxyl and phosphonic acids are deprotected, leading to **pTAM** and **dFT**.

alongside with **dFT-(OMe)$_3$** (63%). Then, the phosphonic acid was deprotected by TMSBr in DCM, and the methyl esters hydrolyzed using lithium hydroxide in 1,4-dioxane/water leading to **pTAM** in 95% yield after purification on a C18 column. **dFT-(OMe)$_3$** was also hydrolyzed, leading to dFT in 99% yield with no purification needed. The relatively low conversion of **dFT** to the monophosponated ester is compensated by the recovery of the starting material. The calculated yield based on the recovery of the starting material reaches 92%. Our large scale synthesis allowed for the selective mono-phosphorylation of **dFT** in 4 steps and two purifications. The key step is the nucleophilic quenching of the trityl cation by trimethyl phosphite leading to the mono-phosphonated derivative.

The extraction of pO_2, pH, and [P_i] from the spectrum can be achieved using spectral fitting of the whole spectrum (see Fig. 1B, top) or only the high or low field EPR lines (Fig. 1B, bottom) using a homemade MATLAB algorithm as reported previously.[18,19] However, to provide a user-friendly interface for those unfamiliar with MATLAB, we developed a graphical user interface for fitting the spectra and deriving the values for pO_2, pH, and [P_i]. Fig. 3 demonstrates the use of the standalone application to fit a spectrum of **pTAM** administered into the mammary gland of a MMTV-PyMT mouse (see ESI† for calibration and use of the app).

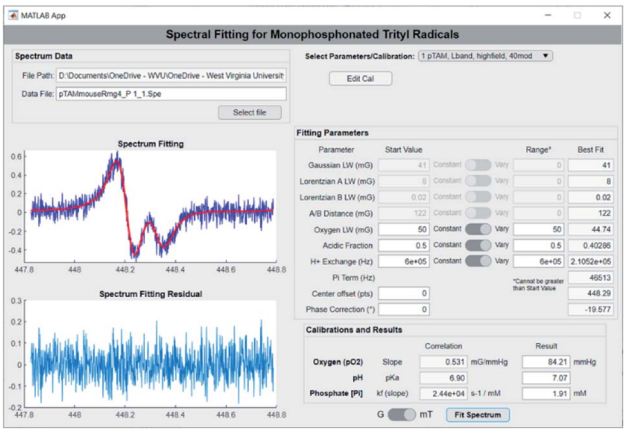

Fig. 3 Screenshot of the **pTAM** spectrum fitting app developed in-house with a spectrum measured of **pTAM** injected directly in the mammary gland of a MMTV-PyMT mouse. Values of pO_2 = 84.21 mmHg, pH = 7.07 and [P_i] = 1.91 mM are automatically calculated from the experimental spectrum.

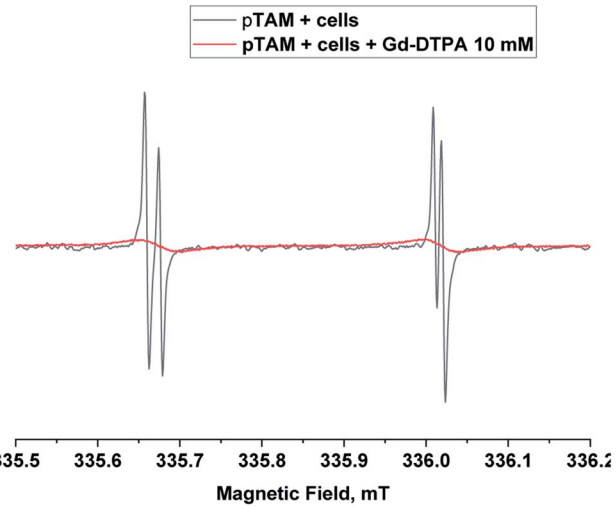

Fig. 4 X-band EPR spectra of **pTAM** (200 μM, 100 μL) incubated with 8.5 × 106 MDA-MB-231 cells without (black) and with 10 mM of Gd-DTPA (red) as extracellular broadening agent.

When applied *in vivo*, the charged nature of the probe and its large size (MW = 1073 g mol^{-1}) is expected to prevent its diffusion through the cell membrane. In order to verify that **pTAM** cannot enter the cytosol, **pTAM** (200 μM) was incubated with 8.5 × 10^6 MDA-MB-231 cells (human triple negative breast cancer cells) with and without 10 mM Gd-DTPA, a paramagnetic extracellular broadening agent.[7] Fig. 4 shows a large broadening of the EPR lines of **pTAM** upon addition of Gd-DTPA and no residual narrow component confirming the absence of **pTAM** spin probe in the intracellular compartment. *In vivo*, the physiological parameters reported by **pTAM** are therefore the extracellular ones.

Next we assessed **pTAM** cell toxicity using the MTT assay for cell viability and proliferation. MDA-MB-231 cells at 60–70% confluency were incubated with various concentration of **pTAM** for 24 h. The result (Fig. 5) shows that up to 1 mM, the probe is

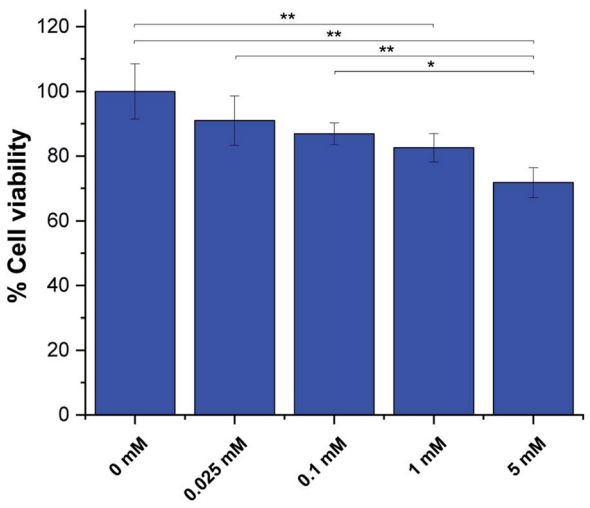

Fig. 5 MTT assays for **pTAM** at various concentration incubated with MDA-MB-231 cells for 24 h. (n = 3, *p < 0.05, **p < 0.01).

well tolerated with ~80% cell viability after 24 h. It is worth noting that only a few hundred micromolar range is required for *in vivo* L-band spectroscopy and the MTT results show no significant difference between 100 μM of probe and the control. Moreover, **pTAM** was incubated 24 h with cells while *in vivo* the probe is cleared from the tissue in less than 1 h.[26] Therefore, the probe can be considered as non-toxic upon local injection, which is the mode of delivery for **pTAM**.[19]

Conclusions

In conclusion, we have reported a procedure to synthesize gram quantities of **pTAM** and a MATLAB application for automatic extraction of pO_2, pH, and $[P_i]$ from an experimental spectrum. Furthermore, we showed that **pTAM** does not cross the cell membrane and has a low cell toxicity for local delivery.

Author contributions

B. D. conceived, supervised the project, performed the experiment and wrote the manuscript. T. D. G. developed the app, performed the MTT assay and wrote the manuscript, M. P. performed the synthesis and wrote the manuscript. S. D. developed the fitting algorithm. M. G. performed the cell and animal work, E. H. H. performed the animal work. T. D. E. supervised and discussed the cell and animal work. V. V. K. provided guidance on the fitting of **pTAM** radical and provided the initial fitting function. All authors have read and edited the manuscript.

Conflicts of interest

There are no conflicts to declare.

Acknowledgements

This work was partially supported by the NIH grants (USA): EB023990, EB028553, CA194013, CA192064, GM104942. The content is solely the responsibility of the authors and does not necessarily represent the official views of the NIH. West Virginia University Health Sciences Center is acknowledged for start-up fund to B. D. Andrey A. Bobko is acknowledged for sharing the initial MATLAB fitting function of pTAM.

Notes and references

1 V. V. Khramtsov, A. A. Bobko, M. Tseytlin and B. Driesschaert, *Anal. Chem.*, 2017, **89**, 4758–4771.
2 J. R. Biller and J. E. McPeak, *Appl. Magn. Reson.*, 2021, 1–27, DOI: 10.1007/s00723-020-01304-z.
3 I. Gertsenshteyn, M. Giurcanu, P. Vaupel and H. Halpern, *J. Physiol.*, 2021, **599**, 1759–1767.
4 B. Epel, S. V. Sundramoorthy, M. Krzykawska-Serda, M. C. Maggio, M. Tseytlin, G. R. Eaton, S. S. Eaton, G. M. Rosen, J. P. Y. Kao and H. J. Halpern, *J. Magn. Reson.*, 2017, **276**, 31–36.
5 J. H. Ardenkjær-Larsen, I. Laursen, I. Leunbach, G. Ehnholm, L. G. Wistrand, J. S. Petersson and K. Golman, *J. Magn. Reson.*, 1998, **133**, 1–12.
6 U. Sanzhaeva, M. Poncelet, O. Tseytlin, M. Tseytlin, M. Gencheva, T. D. Eubank, V. V. Khramtsov and B. Driesschaert, *J. Org. Chem.*, 2020, **85**, 10388–10398.
7 V. Marchand, P. Levêque, B. Driesschaert, J. Marchand-Brynaert and B. Gallez, *Magn. Reson. Med.*, 2017, **77**, 2438–2443.
8 B. Driesschaert, V. Marchand, P. Levêque, B. Gallez and J. Marchand-Brynaert, *Chem. Commun.*, 2012, **48**, 4049–4051.
9 Y. Liu, Y. Song, A. Rockenbauer, J. Sun, C. Hemann, F. A. Villamena and J. L. Zweier, *J. Org. Chem.*, 2011, **76**, 3853–3860.
10 X. Tan, K. Ji, X. Wang, R. Yao, G. Han, F. A. Villamena, J. L. Zweier, Y. Song, A. Rockenbauer and Y. Liu, *Angew. Chem., Int. Ed.*, 2020, **59**, 928–934.
11 M. Poncelet and B. Driesschaert, *Angew. Chem., Int. Ed.*, 2020, **59**, 16451–16454.
12 B. Driesschaert, A. A. Bobko, V. V. Khramtsov and J. L. Zweier, *Cell Biochem. Biophys.*, 2017, **75**, 241–246.
13 C. Rizzi, A. Samouilov, V. Kumar Kutala, N. L. Parinandi, J. L. Zweier and P. Kuppusamy, *Free Radicals Biol. Med.*, 2003, **35**, 1608–1618.
14 V. K. Kutala, N. L. Parinandi, J. L. Zweier and P. Kuppusamy, *Arch. Biochem. Biophys.*, 2004, **424**, 81–88.
15 Y. Liu, F. A. Villamena, Y. Song, J. Sun, A. Rockenbauer and J. L. Zweier, *J. Org. Chem.*, 2010, **75**, 7796–7802.
16 Y. Liu, F. A. Villamena, A. Rockenbauer and J. L. Zweier, *Chem. Commun.*, 2010, **46**, 628–630.
17 I. Dhimitruka, A. A. Bobko, T. D. Eubank, D. A. Komarov and V. V. Khramtsov, *J. Am. Chem. Soc.*, 2013, **135**, 5904–5910.
18 A. A. Bobko, I. Dhimitruka, J. L. Zweier and V. V. Khramtsov, *Angew. Chem., Int. Ed.*, 2014, **53**, 2735–2738.
19 A. A. Bobko, T. D. Eubank, B. Driesschaert, I. Dhimitruka, J. Evans, R. Mohammad, E. E. Tchekneva, M. M. Dikov and V. V. Khramtsov, *Sci. Rep.*, 2017, **7**, 41233.
20 A. Taguchi, S. DeVience, B. Driesschaert, V. V. Khramtsov and H. Hirata, *Analyst*, 2020, **145**, 3236–3244.
21 C. Decroos, T. Prangé, D. Mansuy, J.-L. Boucher and Y. Li, *Chem. Commun.*, 2011, **47**, 4805–4807.
22 O. Y. Rogozhnikova, V. G. Vasiliev, T. I. Troitskaya, D. V. Trukhin, T. V. Mikhalina, H. J. Halpern and V. M. Tormyshev, *Eur. J. Org. Chem.*, 2013, **2013**, 3347–3355.
23 I. Dhimitruka, M. Velayutham, A. A. Bobko, V. V. Khramtsov, F. A. Villamena, C. M. Hadad and J. L. Zweier, *Bioorg. Med. Chem. Lett.*, 2007, **17**, 6801–6805.
24 I. Dhimitruka, O. Grigorieva, J. L. Zweier and V. V. Khramtsov, *Bioorg. Med. Chem. Lett.*, 2010, **20**, 3946–3949.
25 J. J. Jassoy, A. Berndhäuser, F. Duthie, S. P. Kühn, G. Hagelueken and O. Schiemann, *Angew. Chem., Int. Ed.*, 2017, **56**, 177–181.
26 A. A. Gorodetskii, T. D. Eubank, B. Driesschaert, M. Poncelet, E. Ellis, V. V. Khramtsov and A. A. Bobko, *Sci. Rep.*, 2019, **9**, 12093.